Pure Rotational Spectra, Structures, and Hyperfine Constants of OC−AuX (X = F, Cl, Br)

Corey J. Evans,† Linda M. Reynard,‡ and Michael C. L. Gerry*

Department of Chemistry, The University of British Columbia, 2036 Main Mall, Vancouver, British Columbia, Canada V6T 1Z1

Received April 26, 2001

Rotational spectra of OC−AuX (X = F, Cl, Br) have been measured in the frequency range 5−21 GHz, using a pulsed jet cavity Fourier transform microwave spectrometer. The molecules were prepared by ablating Au metal with a Nd:YAG laser and allowing the vapor to react with CO plus a halide precursor contained in the Ar backing gas of the jets. For OC−AuCl and OC−AuBr these are the first high-resolution spectroscopic measurements; for OC−AuF these are the first observations of any kind. All three molecules are linear. Rotational constants, centrifugal distortion constants, and nuclear quadrupole coupling constants have been precisely evaluated. The geometries determined for all three molecules show CO bond lengths close to that of free CO, plus relatively long Au−C bonds. These results are corroborated by ab initio calculations, which have also produced Mulliken populations showing significant σ-donation from CO to Au, plus some π-back-donation from Au to CO. There are major changes in the Au, Cl, and Br nuclear quadrupole coupling constants when CO bonds to AuX, consistent with the formation of strong Au−C bonds. The structural properties of OC−AuF are somewhat different from those of OC−AuCl and OC−AuBr.

Introduction

Carbon monoxide is one of the most important ligands in all coordination chemistry. There are so many carbonyl complexes, and their reactions are so numerous, that standard textbooks can deal with only a selection, particularly of the latter.[1,2] There are mono- and polynuclear metal carbonyls, both with and without bridging groups. Metal carbonyls are used, or are intermediates, in many catalytic reactions, such as hydroformylation of alkenes to aldehydes or production of acetic acid from methanol.[2,3] Carbon monoxide poisoning in mammals is the result of formation of an Fe−CO complex.

The vast majority of carbonyl complexes is found for the metals of groups 5−10. For these the standard picture of the bonding of nonbridging carbonyls involves σ-donation to the metal from a slightly antibonding orbital on CO,[4] along with π-back-donation from a metal d-orbital to a π*-antibonding orbital on CO. According to this picture, the latter predominates, and the CO bonding is weakened. This idea is used to rationalize a decrease (a red shift) in the CO stretching frequency from that of monomeric CO (2138 cm^{-1} [5]).[1,2,6] Commonly observed short M−C distances (M = metal), plus apparent increases of the CO bond length over that of free CO (r_e = 1.128 Å [5]), are consistent with this view.[2,7]

The metals at the edges of the d-block (groups 3, 4, 11, and 12) have few known carbonyl complexes. Of the coinage metals (group 11), Cu has a moderate number, while Ag and Au have very few.[6,8,9] Only recently have compounds containing homoleptic cations of the type $M(CO)_2^+$ been prepared for M = Ag and Au.[6,9,10] Compounds containing these ions are often isolated only when the acidity of the metal ion is increased using a bulky "weakly coordinating anion".[6,9] An important feature of these ions is that their CO stretching frequencies are *increased* (blue shifted) from those of free CO. Also, X-ray crystallography has shown the M−C bonds to be relatively long and the C−O bonds quite short (though librational effects reduce the reliability of the values obtained).[6] Both the stretching frequencies and bond lengths have been rationalized in terms of severely reduced, even negligible, π-back-bonding to CO.[6]

This paper is the first on the Fourier transform microwave (FTMW) spectra of a series of complexes of general formula OC−MX, with M = Cu, Ag, and Au and X = F, Cl, and Br. The work was prompted by our recent studies of the spectra of corresponding complexes of formula Ng−MX, with Ng = Ar and Kr.[11−15] These complexes have been found to have short Ng−M Bonds, high Ng−M bond energies (D_e(Kr−Au) ∼ 70

* Corresponding author. Phone: (604) 822-2464. Fax: (604) 822-2847. E-mail: mgerry@chem.ubc.ca.

† Present address: Department of Chemistry, University of Kentucky, Lexington, KY 40506-0055.

‡ Present address: Department of Chemistry, University of Toronto, 80 St. George Street, Toronto, Ontario, Canada M5S 3H6.

(1) Huheey, J. E.; Keiter, E. A.; Keiter, R. L. *Inorganic Chemistry*, 4th ed.; Harper Collins: New York, 1993.
(2) Cotton, F. A.; Wilkinson, G.; Murillo, C. A.; Bachmann, M. *Advanced Inorganic Chemistry*, 6th ed.; Wiley: New York, 1999.
(3) Parshall, G. W.; Ittel, S. D. *Homogeneous Catalysis: The Application and Chemistry of Soluble Transition Metal Complexes*, 2nd ed.; Wiley: New York, 1992.
(4) DeKock, R. L.; Sarapu, A. C.; Fenske, R. F. *Inorg. Chem.* **1971**, *10*, 38.
(5) Huber, K. P.; Herzberg, G. *Molecular Spectra and Molecular Structure: Constants of Diatomic Molecules*; Van Nostrand: New York, 1979.
(6) Hurlburt, P. K.; Rock, J. J.; Luck, J. S.; Dec, S. F.; Webb, J. D.; Anderson, O. P.; Strauss, S. H. *J. Am. Chem. Soc*. **1994**, *116*, 10003.
(7) Shriver, D. F.; Atkins, P.; Lanford, C. H. *Inorganic Chemistry*, 2nd ed.; Freeman: New York, 1994.
(8) Wilkinson, G., Ed. *Comprehensive Coordination Chemistry*; Pergamon: Oxford, U.K., 1987; Vol. 5: (a) Hathaway, B. J. *Copper*; pp 553−774. (b) Lancashire, R. J. *Silver*; pp 777−859. (c) Puddephatt, R. J. *Gold*; pp 862−923.
(9) Willner, H.; Schaebs, J.; Hwang, G.; Mistry, F.; Jones, R.; Trotter, J.; Aubke, F. *J. Am. Chem. Soc.* **1992**, *114*, 8972.
(10) Weber, L. *Angew. Chem., Int. Ed. Engl.* **1994**, *33*, 1077.
(11) Evans, C. J.; Gerry, M. C. L. *J. Chem. Phys.* **2000**, *112*, 1321.
(12) Evans, C. J.; Gerry, M. C. L. *J. Chem. Phys.* **2000**, *112*, 9363.
(13) Evans, C. J.; Lesarri, A.; Gerry, M. C. L. *J. Am. Chem. Soc*. **2000**, *122*, 6100.

10.1021/ic0104407 CCC: $20.00
Published on Web 10/17/2001

kJ mol^{-1} for Kr−AuCl), and high Ng−M stretching frequencies (ν(Kr−Au) ∼ 170 cm^{-1} for Kr−AuCl). There are also significant changes in the Cu and Au nuclear quadrupole coupling constants (NQCC) on complex formation. These results, combined with results from ab initio calculations, including Mulliken orbital population analyses, are consistent with weak chemical bonding between the noble gas and Cu or Au, in which the noble gas acts as a weak Lewis base. Clearly the carbonyl coinage metal halides are strong candidates for similar studies.

There are reports in the literature of only three OC−MX complexes, namely OC−AuCl, OC−AuBr, and OC−CuCl. Of these OC−AuCl has been known the longest. It was first isolated in 1925 by Kharasch and Isbell,[16] who passed CO over gold chloride at 100 °C; more recently the yield has been improved by using thionyl chloride as a medium.[17] Browning et al. recorded and assigned its infrared and Raman spectra (50−3000 cm^{-1}) in solution, as well as the Raman spectrum of the solid.[18] In two other infrared studies only the CO stretching frequency was measured. All studies showed ν(CO) ∼ 2160 cm^{-1}, considerably greater than that of free CO.[17−19] The crystal structure has been determined by Jones.[20] The crystals contain discrete linear OC−AuCl molecules, with the shortest contacts between molecules being 3.38 Å. The O−C bond length was found to be short (1.11 Å), but again librational effects may reduce its accuracy. Mössbauer spectra of several Au(I) complexes have been measured;[21] for OC−AuCl the NQCC of Au was estimated as (−)916 MHz.

The complex OC−AuBr has only recently been isolated.[19] It has been found to be rather unstable. Its CO stretching frequency is very close to that of OC−AuCl.

Though aqueous acidic CuCl has long been known to absorb CO and was used to assay CO gas,[8a] it is only recently that the resulting complex, OC−CuCl, has been isolated as a solid well enough to determine its crystal structure. The crystal contains chlorine-bridged layers with Cu(I) roughly tetrahedrally coordinated.[22] The CO stretching frequency (2127 cm^{-1}) is slightly lower than that of free CO. However, monomeric OC−CuCl has also been isolated in an Ar matrix; in this case ν(CO) ∼ 2157 cm[1], somewhat bigger than that of free CO.[23]

To investigate the stability of the three chlorides OC−MCl (M = Cu, Ag, Au), Antes et al.[24] carried out an extensive series of ab initio calculations, using relativistic core potentials for the metals. They predicted geometries, dissociation energies, stretching force constants, dipole moments, and ^{35}Cl nuclear quadrupole coupling constants. In addition they predicted sizable π-back-donation from the metal to a π^* orbital of CO. This result, which has been corroborated by a more recent calculation,[25] contradicts the simple idea that the blue shift of the CO stretching frequency from that of free CO indicates no π-back-bonding.[6] Antes et al. suggest instead that the blue shift may have an electrostatic origin.

This paper reports the detection and measurement of the pure rotational spectra of OC−AuF, OC−AuCl, and OC−AuBr. This is the first high-resolution spectroscopic study of OC−AuCl and OC−AuBr and the first observation of any kind of OC−AuF. In each case the samples have been prepared by laser ablation of Au in the presence of CO and a halogen precursor and stabilized in the gas phase in a supersonic jet of Ar. The spectra were measured with a cavity-pulsed FTMW spectrometer. Rotational constants, centrifugal distortion constants, nuclear quadrupole coupling constants, and nuclear spin-rotation coupling constants have been obtained. A major aim has been to determine the bond lengths, particularly the CO distance, free of librational effects, which should help in our understanding of the bonding in the molecules. Since the ab initio results in the literature refer only to OC−AuCl,[24,25] we have carried out corresponding calculations for all three complexes.

Experimental Methods

The spectra were observed with the Balle−Flygare[26] type pulsed-jet spectrometers and associated laser ablation systems which have been described in detail earlier.[27−29] Briefly, each spectrometer cell consists of a Fabry−Perot cavity employing two spherical aluminum mirrors 28 cm diameter, with a radius of curvature 38.4 cm, held approximately 30 cm apart. One mirror is fixed, while the other can be moved to tune the cavity to the desired polarization frequency. The pulsed supersonic jet containing the sample is injected into the cavity via a General Valve (Series 9) nozzle, which is mounted slightly off-center in the fixed mirror. Although this "parallel" arrangement optimizes both the sensitivity and resolution of the spectrometer, it also causes all lines to be doubled by the Doppler effect because the direction of the jet is parallel to that of the microwave propagation. The line frequency is obtained by taking the average of the two Doppler components.

The frequency range of the present experiments was 5−21 GHz. Frequency measurements were referenced to a Loran frequency standard accurate to 1 part in 10^{10}. Observed line widths were ∼7−10 kHz (FWHM), and the line frequencies were estimated to be accurate to ±1 kHz.

Mounted in the fixed mirror are the pulsed nozzle and ablation system.[29] A metal rod is placed ∼5 mm from the orifice of the nozzle. The rod is ablated by irradiating it with a Nd:YAG laser (in the present experiments, the 2nd harmonic, 532 nm). The resulting metal plasma then reacts with the gas sample which is pulsed (at a repetition rate of 1 Hz) into the reaction region. To allow a fresh surface of the metal to be exposed for each laser pulse the metal rod is continuously rotated and translated. The gas sample is then supersonically expanded into the cavity via a 5 mm diameter nozzle. The sample molecules are stabilized in the essentially collision-free environment of the jet. Rotational temperatures achieved are believed to be ∼3 K.

In the present experiments a gold rod or a small piece of gold foil wrapped around a glass rod was used (99.999% purity). The precursors were Cl_2, Br_2, or SF_6 (0.1%) and 0.2−1.5% of CO (Praxair) in Ar at a backing pressure of ∼6 bar. A 1.5% concentration of CO was found to give the strongest signal. For the ^{13}C and ^{18}O isotopomers the following isotopically enriched samples were used: ^{13}CO 99.2% (with 14.6% ^{18}O), Matheson; ^{13}CO 99.0% (with ∼10% ^{18}O), Cambridge Isotopes Laboratory; ^{12}CO 72% (with 28% ^{18}O), Icon Inc. The strongest lines from OC−AuCl were easily seen in 150 pulses while those from OC−AuBr and OC−AuF were weaker and required longer sampling times to obtain a usable signal. The OC−AuI complex was not

(14) Evans, C. J.; Rubinoff, D. S.; Gerry, M. C. L. *Phys. Chem. Chem. Phys.* **2000**, *2*, 3943.
(15) Reynard, L. M.; Evans, C. J.; Gerry, M. C. L. *J. Mol. Spectrosc.* **2001**, *206*, 33.
(16) Kharasch, M. S.; Isbell, M. S. *J. Am. Chem. Soc.* **1930**, *52*, 2919.
(17) Dell'Amico, D.; Calderazzo, F. *Gazz. Chim. Ital.* **1973**, *103*, 1099.
(18) Browning, J.; Goggin, P. L.; Goodfellow, R. J.; Norton, M. G.; Rattray, A. J. M.; Taylor, B. F.; Mink, J. *J. Chem. Soc., Dalton Trans.* **1977**, 2061.
(19) Dell'Amico, D.; Calderazzo, F.; Robino, P.; Segre, A. *J. Chem. Soc., Dalton Trans.* **1991**, 3017.
(20) Jones, P. G. *Z. Naturforsch., B* **1982**, *37*, 823.
(21) Jones, P. G.; Maddock, A. G.; Mays, M. J.; Muir, M. M.; Williams, A. F. *J. Chem. Soc., Dalton Trans.* **1977**, 1434.
(22) Hakansson, M.; Jagner, S. *Inorg. Chem.* **1990**, *29*, 5241.
(23) Plitt, H. S.; Bär, M. R.; Ahlrichs, R.; Schnöckel, H. *Inorg. Chem.* **1992**, *31*, 463.
(24) Antes, I.; Dapprich, S.; Frenking, G.; Schwerdtfeger, P. *Inorg. Chem.* **1996**, *35*, 2089.
(25) Fortunelli, A.; Germano, G. *J. Phys. Chem. A* **2000**, *104*, 10834.
(26) Balle, T. J.; Flygare, W. H. *Rev. Sci. Instrum.* **1981**, *52*, 33.
(27) Xu, Y.; Jäger, W.; Gerry, M. C. L. *J. Mol. Spectrosc.* **1992**, *151*, 206.
(28) Brupbacher, Th.; Bohn, R. K.; Jäger, W.; Gerry, M. C. L.; Pasinszki, T.; Westwood, N. P. C. *J. Mol. Spectrosc.* **1997**, *181*, 316.
(29) Walker, K. A.; Gerry, M. C. L. *J. Mol. Spectrosc.* **1997**, *182*, 178.

Table 1. Molecular Constants of OC−Au^{35}Cl and OC−Au^{37}Cl[a]

	$^{16}O^{12}C-Au^{35}Cl$		
params	$v = 0$	$v = 1$	$v = 2$
B_v	1404.542 435(55)	1401.710 728(78)	1398.874 971(86)
$10^5 D_{Jv}$	7.20(13)	7.34(17)	7.52(19)
eQq(Au)	−1025.9753(29)	−1022.683(12)	−1019.388(13)
eQq(Cl)	−36.3884(34)	−36.5322(66)	−36.6676(72)
$10^4 C_l$(Au)	8.55(130)	8.33(237)	7.75(250)

	$^{16}O^{12}C-Au^{37}Cl$		$^{16}O^{13}C-Au^{35}Cl$	
params	$v = 0$	$v = 1$	$v = 0$	$v = 1$
B_v	1368.397 874(63)	1365.655 001(81)	1390.474 073(77)	1387.676 049(76)
$10^5 D_{Jv}$	6.92(14)	6.98(18)	7.12(17)	7.17(17)
eQq(Au)	−1026.0802(41)	−1022.837(13)	−1026.370(11)	−1023.126(12)
eQq(Cl)	−28.6895(62)	−28.7915(71)	−36.3800(67)	−36.5218(66)
$10^4 C_l$(Au)	8.45(144)	9.61(237)	9.46(227)	6.83(225)

	$^{16}O^{13}C-Au^{37}Cl$		$^{18}O^{12}C-Au^{35}Cl$	$^{18}O^{13}C-Au^{35}Cl$
params	$v = 0$	$v = 1$	$v = 0$	$v = 0$
B_v	1354.808 515(82)	1352.101 168(82)	1336.248 158(87)	1323.818 69(91)
$10^5 D_{Jv}$	6.92(18)	6.89(18)	6.36(19)	6.43(20)
eQq(Au)	−1026.499(13)	−1023.272(12)	−1026.084(14)	−1026.483(14)
eQq(Cl)	−28.6726(72)	−28.7912(73)	−36.3803(74)	−36.3714(74)
$10^4 C_l$(Au)	4.97(248)	9.33(24)	5.71(204)	8.02(264)

[a] Numbers in parentheses are one standard deviation in units of the last significant figure.

investigated because of a problem in finding an iodide precursor which would allow us to obtain usable signals.[30]

Theoretical Calculations

The geometries of CO, AuX, and OC−AuX (X = F, Cl, Br) were optimized at the second-order Møller−Plesset (MP2)[31] level of theory using the GAUSSIAN 98 suite of programs.[32] For Au a relativistic core potential (RECP) was used.[33] The basis set used for Au was a (9s/7p/6d/3f) Gaussian basis set contracted to (8s/4p/5d/3f).[33,34] For O, C, and F we used the 6-311G** basis set.[32] For Cl we used the (631111s/52111p) McLean−Chandler basis set[35] augmented with one d-polarization function ($\alpha_d = 0.75$).[24] For Br we used the aug-cc-pVTZ basis set.[36]

Results and Analysis

An initial geometry for OC−AuCl was taken from the theoretical study of Antes et al.;[24] their MP2 (relativistic) values were used. This geometry was modified by approximating the Au−Cl bond length to the r_e of monomeric AuCl,[37] following the results for Kr−AuCl and Ar−AuCl.[13] As the C−O distance should not change appreciably on coordination, the major uncertainty was in the C−Au distance and resulted in an optimal search range of ±300 MHz for $J = 3-2$. Lines were found within 200 MHz of the predicted frequency and were tentatively assigned to the major isotopomer, $^{16}O^{12}C-Au^{35}Cl$, in the ground vibrational state ($v = 0$). Hyperfine structure due to both Au and Cl was assigned. Further lines were found at 2800 MHz intervals, indicating that they were from a linear molecule. The overall assignment was confirmed by the prediction and observation of corresponding lines from $^{16}O^{12}C-Au^{37}Cl$. Additional confirmation of the assignment was made from the ratio of the observed nuclear quadrupole coupling constants (NQCC) of ^{35}Cl and ^{37}Cl, which was in excellent agreement with the ratio of their nuclear quadrupole moments.

Using the ^{13}C isotopically enriched CO, lines from $^{16}O^{13}C-Au^{35}Cl$ were found and assigned to the ground vibrational state ($v = 0$). However initial determination of the structure produced a C−Cl distance 0.2 Å longer than that predicted by Antes et al.[24] This discrepancy initiated a search for lines from excited vibrational states. A thorough search revealed that the original lines were from a $v = 1$ state and not the originally assigned $v = 0$ state. On reassignment the C−Cl distance agreed well with the theoretical and earlier experimental values. In all, lines were measured and assigned to the $v = 0$, 1, and 2 vibrational states of $^{16}O^{12}C-Au^{35}Cl$, $v = 0$ and 1 vibrational states of $^{16}O^{12}C-Au^{37}Cl$, $^{16}O^{13}C-Au^{35}Cl$, and $^{16}O^{13}C-Au^{37}Cl$, and $v = 0$ vibrational state of $^{18}O^{12}C-Au^{35}Cl$ and $^{18}O^{13}C-Au^{35}Cl$.

The measured frequencies were fitted using Pickett's weighted least-squares program SPFIT.[38] The Hamiltonian was

$$\mathbf{H} = \mathbf{H}_{rot} + \mathbf{H}_{nucl.\ quad.} + \mathbf{H}_{spin-rot} \quad (1)$$

where

$$\mathbf{H}_{rot} = B_v \mathbf{J}^2 - D_{Jv} \mathbf{J}^4 \quad (2)$$

$$\mathbf{H}_{nucl.\ quad.} = -\frac{1}{6}(\mathbf{V}_{Au}^{(2)}\mathbf{Q}_{Au}^{(2)} + \mathbf{V}_{X}^{(2)}\mathbf{Q}_{X}^{(2)}) \quad (3)$$

$$\mathbf{H}_{spin-rot} = C_l(\mathrm{Au})\mathbf{I}_{Au}\cdot\mathbf{J} + C_l(\mathrm{X})\mathbf{I}_{X}\cdot\mathbf{J} \quad (4)$$

where X in eqs 3 and 4 refers to the halogen. The line frequencies were assigned quantum numbers using the $\mathbf{F}_1 = \mathbf{I}_{Au} + \mathbf{J}$ and $\mathbf{F} = \mathbf{I}_{Cl} + \mathbf{F}_1$ coupling scheme, where Au and both isotopes of Cl have a nuclear spin (I) of 3/2. The fitted molecular constants, including rotational constants, centrifugal distortion constants, and nuclear quadrupole coupling constants, are listed in Table 1. The line frequencies and their assignments are given

(30) Reynard, L. M.; Evans, C. J.; Gerry, M. C. L. *J. Mol. Spectrosc.* **2001**, *205*, 344.
(31) Møller, C.; Plesset, M. S. *Phys. Rev.* **1934**, *46*, 618.
(32) Frisch, M. J.; et al. *Gaussian 98, Revision A.9*; Gaussian, Inc: Pittsburgh, PA, 1998.
(33) Schwerdtfeger, P. *Chem. Phys. Lett.* **1991**, *183*, 457.
(34) Schwerdtfeger, P.; Dolg, M.; Schwarz, W. H. E.; Bowmaker, G. A.; Boyd, P. D. W. *J. Chem. Phys.* **1989**, *91*, 1762.
(35) McLean, A.; Chandler, G. S. *J. Chem. Phys.* **1980**, *72*, 5639.
(36) Wilson, A. K.; Woon, D. E.; Peterson, K. A.; Dunning, T. H., Jr. *J. Chem. Phys.* **1999**, *110*, 7667.
(37) Evans, C. J.; Gerry, M. C. L. *J. Mol. Spectrosc.* **2000**, *203*, 105.
(38) Pickett, H. M. *J. Mol. Spectrosc.* **1991**, *148*, 371.

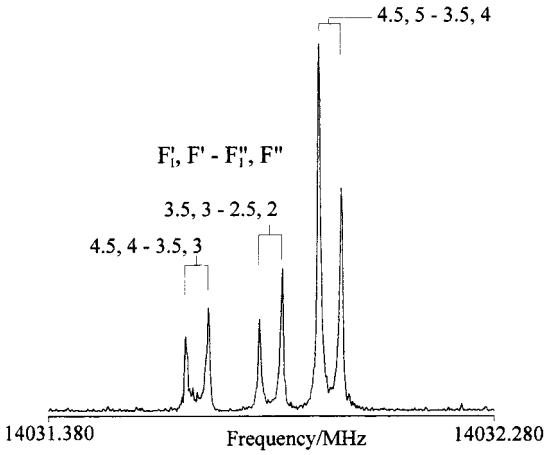

Figure 1. Portion of the hyperfine structure of the $J = 5-4$ transition of $^{16}O^{12}C-Au^{35}Cl$ in the ground vibrational state. Experimental conditions: 1.5% CO with 0.1% Cl_2 in Ar at a backing pressure of ~6 atm.; Au rod; 8 K transform; 150 averaging cycles.

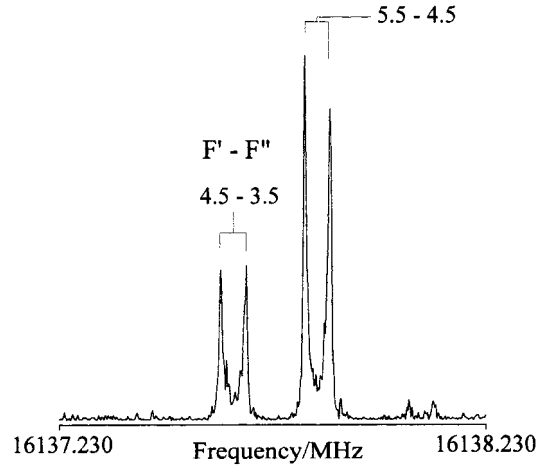

Figure 2. Portion of the hyperfine structure of the $J = 4-3$ transition of $^{16}O^{13}C-AuF$ in the ground vibrational state. Experimental conditions: 1.5% ^{13}CO with 0.1% SF_6 in Ar at a backing pressure of ~6 atm.; Au rod; 8 K transform; 300 averaging cycles.

Table 2. Molecular Constants of OC−AuF[a]

params	$^{16}O^{12}C-AuF$	$^{16}O^{13}C-AuF$	$^{18}O^{12}C-AuF$
B_0	2040.008 587(86)	2016.241 283(99)	1915.731 59(10)
10^4D_J	1.4209(225)	1.4174(252)	1.260(30)
eQq(Au)	−1006.2852(21)	−1006.5920(45)	−1006.2847(45)
10^3C_I(Au)	1.068(160)	1.131(218)	1.167(243)

[a] Numbers in parentheses are one standard deviation in units of the last significant figure.

as Supporting Information. A portion of the $J = 5-4$ transition of $OC-Au^{35}Cl$ is depicted in Figure 1.

Using the geometries determined for the Ar−AuX (X = F, Cl, Br) complexes and then scaling the bond distances determined for OC−AuCl (see below), we estimated the structures of OC−AuF and OC−AuBr and predicted their pure rotational spectra. For OC−AuF, lines were found around 8160 MHz (within 200 MHz of the predicted frequency) and assigned to the $v = 0$ state of $^{16}O^{12}C-AuF$. This assignment was confirmed by the prediction and observation not only of further transitions but also of lines from the $v = 0$ state of $^{16}O^{13}C-AuF$ and $^{18}O^{12}C-AuF$. An example transition is depicted in Figure 2. No lines from excited vibrational states were observed. The fitted molecular constants are given in Table 2. Since the observed hyperfine structure was due only to Au, the coupling scheme used was $\mathbf{F} = \mathbf{I}_{Au} + \mathbf{J}$. Line frequencies and their assignments are given in the Supporting Information.

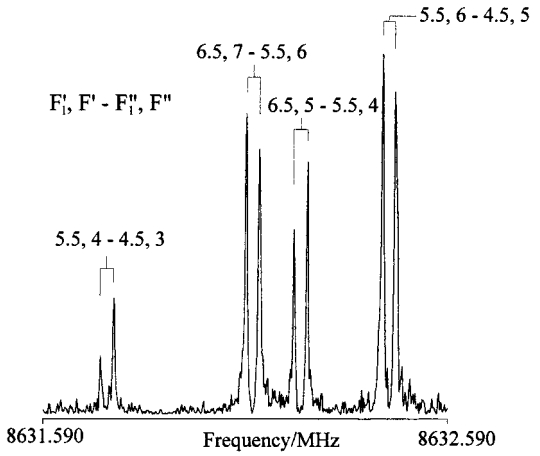

Figure 3. Portion of the hyperfine structure of the $J = 5-4$ transition of $^{16}O^{12}C-Au^{81}Br$ in the ground vibrational state. Experimental conditions: 1.5% CO with 0.1% Br_2 in Ar at a backing pressure of ~6 atm; Au rod; 8 K transform; 1000 averaging cycles.

Table 3. Molecular Constants of OC−$Au^{79}Br$ and OC−$Au^{81}Br$[a]

params	$^{16}O^{12}C-Au^{79}Br$	$^{16}O^{13}C-Au^{79}Br$	$^{18}O^{12}C-Au^{79}Br$
B_0	874.074 043(56)	866.388 848(56)	840.671 113(82)
10^5D_J	3.492(69)	3.385(71)	3.228(98)
eQq(Au)	−999.119(23)	−999.560(22)	−999.320(44)
eQq(^{79}Br)	285.0567(176)	284.9758(164)	284.997(23)
10^4C_I(^{79}Br)	7.72(159)	6.43(157)	7.72[b]
params	$^{16}O^{12}C-Au^{81}Br$	$^{16}O^{13}C-Au^{81}Br$	$^{18}O^{12}C-Au^{81}Br$
B_0	862.657 385(56)	855.086 429(59)	829.866 842(79)
10^5D_J	3.387(68)	3.293(72)	2.969(95)
eQq(Au)	−999.134(23)	−999.543(23)	−999.323(41)
eQq(^{81}Br)	238.1183(172)	238.0749(179)	238.092(23)
10^4C_I(^{81}Br)	7.80(161)	6.88(166)	7.80[c]

[a] Numbers in parentheses are one standard deviation in units of the last significant figure. [b] Fixed to the OC−$Au^{79}Br$ value. [c] Fixed to the OC−$Au^{81}Br$ value.

For OC−AuBr, lines of $J = 5-4$ were found around 8630 MHz (within 100 MHz of the predicted frequency) and were assigned to the $v = 0$ vibrational state of $^{16}O^{12}C-Au^{81}Br$ on the basis of the NQCC of Br. The assignment was confirmed by the prediction and observation of lines from the $v = 0$ state of $^{16}O^{12}C-Au^{79}Br$. Further confirmation of the assignment was made from the ratio of the observed NQCC of ^{79}Br and ^{81}Br, which agreed well with the ratio of their quadrupole moments. Weak overlapping lines, presumably from excited vibrational states, were observed but could not be assigned. In all, lines were measured and assigned to the $v = 0$ state of $^{16}O^{12}C-Au^{79}Br$, $^{16}O^{12}C-Au^{81}Br$, $^{16}O^{13}C-Au^{79}Br$, $^{16}O^{13}C-Au^{81}Br$, $^{18}O^{12}C-Au^{79}Br$, and $^{18}O^{12}C-Au^{81}Br$. An example for $^{16}O^{12}C-Au^{81}Br$ is given in Figure 3. The derived molecular constants are in Table 3. The line frequencies and their assignments are once again presented as Supporting Information. The $\mathbf{F}_1 = \mathbf{I}_{Au} + \mathbf{J}$ and $\mathbf{F} = \mathbf{I}_{Br} + \mathbf{F}_1$ coupling scheme was employed, where both isotopes of Br have a nuclear spin of 3/2.

Geometries of the Complexes

Microwave spectroscopy is a valuable technique for obtaining geometries of gas-phase molecules. The accurate measurements (±1 kHz in a cavity FTMW spectrometer) produce similarly precise rotational constants and moments of inertia, which in favorable circumstances (usually for diatomic molecules) can

Table 4. Structures of OC−AuX (X = F, Cl, Br) (in Å)[a]

	method	r(C−O)	r(C−Au)	r(Au−X)	Comment
OC−AuCl	MP2[b]	1.141	1.892	2.225	
	MP2[24]	1.141	1.872	2.266	
	X-ray[20]	1.11	1.93	2.261	
	r_0	1.132(2)	1.884(2)	2.217 2(6)	
	r_s	1.132 3	1.882 9	2.215 5	
	$r_{I\epsilon}$	1.132 3(1)	1.882 7(1)	2.215 49(6)	$\epsilon_0 = 0.401(12)$ amu Å^2
	$r_m^{(1)}$	1.131 7(1)	1.881 7(1)	2.214 27(9)	$c = 0.0418(12)$ amu$^{1/2}$ Å
	$r_m^{(2)}$	1.126 501(8)	1.885 93(6)	2.212 489(3)	$c = 0.154\ 18(18)$ amu$^{1/2}$ Å
					$d = 0.469\ 09(74)$ amu$^{1/2}$ Å^2
OC−AuF	MP2[b]	1.142	1.849	1.934	
	r_0	1.134	1.847	1.909	
	r_s	1.133 6			
OC−AuBr	MP2[b]	1.141	1.899	2.350	
	r_0	1.132(1)	1.892(2)	2.337 7(5)	
	r_s	1.1321	1.891 7	2.336 3	
	$r_{I\epsilon}$	1.132 160(5)	1.891 730(6)	2.336 301(4)	$\epsilon_0 = 0.4781(11)$ amu Å^2
	$r_m^{(1)}$	1.131 71(1)	1.890 95(2)	2.335 35(1)	$c = 0.039\ 35(19)$ amu$^{1/2}$ Å
	$r_m^{(2)}$	1.134 1(5)	1.888 6(5)	2.336 4(2)	$c = 0.018(12)$ amu$^{1/2}$ Å
					$d = 0.253(55)$ amu$^{1/2}$ Å^2
AuCl	MP2[b]			2.225	
	r_e [37]			2.199	
AuF	MP2[b]			1.967	
	r_e [42]			1.918	
AuBr	MP2[b]			2.338	
	r_e [37]			2.318	
CO	MP2[b]	1.139			
	r_e [5]	1.128			

[a] Numbers in parentheses are one standard deviation in units of the last significant figure. [b] This work

give bond lengths accurate to $\pm 10^{-6}$ Å or better. Ideally what are needed are equilibrium (r_e) geometries at the potential minima, because these are isotopically independent and provide direct comparison with theory. For the linear OC−AuX molecules, which have three bond lengths, determination of r_e values requires spectra of at least three isotopic species in not only the ground vibrational state but also excited states of *all* normal modes. Since these could not be obtained, geometries which are at best only approximations to the r_e values have been determined, to rather lower accuracies than the experiments would seem to warrant. Several methods have been used.

(a) Ground-State Effective (r_0) Geometries.

For each complex the effective geometries calculated directly from the ground-state rotational constants B_0 in Tables 1−3 were first obtained. In each case the equation used was

$$I_0(j) = I_{in}(j) + \sum_k \left(\frac{\partial I(j)}{\partial P_k}\right)\Delta P_k \qquad (5)$$

where $I_0(j) = h/8\pi^2 B_0(j)$ is the experimental moment of inertia of the jth isotopomer, $I_{in}(j)$ is the corresponding moment from an initial assumed structure, and P_k is the length of the kth bond. For OC−AuF, where there are only three rotational constants (Table 2), an exact calculation was carried out. For OC−AuCl (Table 1) and OC−AuBr (Table 3) least-squares fits were carried out. The results are the r_0 values in Table 4.

(b) Substitution (r_s) Geometries.

The ground-state moments of inertia I_0 have vibrational contributions given by the equation

$$I_0 = I_e(r) + \epsilon_0 \qquad (6)$$

where $I_e(r)$ is the equilibrium moment of inertia and ϵ_0 is the contribution of the zero-point vibrations. Because both I_e and ϵ_0 vary with isotopic species, the r_0 structures also vary with isotopic species and thus have only limited accuracies.

In the substitution (r_s) method an attempt is made to reduce the effect of ϵ_0 by assuming it to be independent of isotopomer and determining atomic positions from changes in I_0 on isotopic substitution.[39] One isotopomer is chosen as the basis molecule, and the position of each atom in this basis is determined from the change in I_0 when it is isotopically substituted. The equation is

$$z_i^2 = \frac{\Delta I}{\mu} \qquad (7)$$

where z_i is the coordinate of the substituted atom i, $\Delta I = I_0(\text{sub}) - I_0(\text{basis})$, and $\mu = M\Delta m/(M + \Delta m)$, with M the mass of the basis molecule and $\Delta m = M(\text{sub}) - M(\text{basis})$.

Table 4 contains also the r_s structures of OC−AuCl and OC−AuBr. Since there is only one isotope of Au, it was located using the first moment condition

$$\sum_i m_i z_i = 0 \qquad (8)$$

where m_i is the mass of the ith atom of the basis molecule. The values given are probably reliable to ±0.005 Å. Since isotopic substitutions in OC−AuF could be made only at C and O, a value could be obtained only for r_s(CO); it is similarly reliable.

(c) Alternative Substitution ($r_{I\epsilon}$) Structures.

An alternative way of minimizing the effect of ϵ_0 in eq 6 is to do a least-squares fit to the geometry and include ϵ_0 as one of the fit parameters (again assuming its isotopic independence). The resulting bond lengths are designated $r_{I\epsilon}$.[40] With enough isotopic substitutions $r_{I\epsilon}$ values and r_s values are equivalent. Listed in Table 4 are $r_{I\epsilon}$ geometries for OC−AuCl and OC−AuBr, which do indeed agree well with the r_s structures.

(39) Costain, C. C. *J. Chem. Phys*. **1958**, *29*, 864.
(40) Rudolph, H. D. *Struct. Chem*. **1991**, *2*, 581.

(d) Mass-Dependent, $r_m^{(1)}$ and $r_m^{(2)}$, Geometries.

In an effort to account for the mass-dependence of ϵ_0, geometries designated $r_m^{(1)}$ and $r_m^{(2)}$ were obtained.[41] The experimental I_0 values were fit to

$$I_0 = I_m(r) + c(I_m)^{1/2} + d(m_1m_2m_3m_4/M)^{1/6} \qquad (9)$$

where M is the sum of the atomic masses m_i of a given isotopomer, c and d are constants, and $I_m(r)$ is the moment of inertia with the resulting bond lengths. The $r_m^{(2)}$ fits used all the terms in eq 9; in the $r_m^{(1)}$ fits d was set to zero. The resulting values for OC−AuCl and OC−AuBr are also in Table 4.

In general $r_m^{(1)}$ and, particularly, $r_m^{(2)}$ structures are considered to produce among the best approximations to the equilibrium geometries of all those calculated here.[41] For OC−AuCl the $r_m^{(2)}$ values appear to be the most precise, with the CO distances very close to the r_e value in CO itself (Table 4). However the corresponding values for OC−AuBr are much less precise, even with a very comparable data set. This suggests that great care should be taken with any physical interpretation. It is also found that for both molecules the $r_m^{(2)}$ bond lengths are highly correlated, with several perfect correlations for OC−AuBr. Part of the problem may arise because no isotopic substitution could be made at Au. As well, the $r_m^{(2)}$ fits were to five parameters using six pieces of data. Evidently in the present situation $r_m^{(2)}$ values are of limited use. The $r_m^{(1)}$ structures add little to those obtained by the other methods.

Fortunately, despite all the difficulties described above, the geometries obtained by different methods for a given molecule are quite self-consistent internally and comparisons can be made, both with geometries from ab initio calculations and with geometries of other molecules.

From Table 4 it is seen that the CO bond lengths (∼1.132 Å for OC−AuCl and OC−AuBr; ∼1.134 Å for OC−AuF) are in good agreement with, though slightly less than, the ab initio values calculated both in the present work and by Antes et al. for OC−AuCl.[24] They are 0.004−0.006 Å greater than the r_e value of CO monomer (1.128 Å [5]) in good agreement with 0.002 Å increase predicted ab initio. For OC−AuCl r(CO) is more than 0.02 Å longer than the value found by Jones[20] using X-ray diffraction. For all three complexes the AuX and CAu distances are within less than 0.05 and 0.01 Å from the ab initio values, respectively. In the complexes r(AuX) differs from the r_e values of the monomers by −0.01, +0.02, and +0.02 Å for X = F, Cl, and Br, respectively.

Table 5 contains comparisons of the values of r(CO) and r(MC) for OC−AuX and several related molecules. Three points stand out: (i) The values for r(CO) in OC−AuX are among the shortest measured for carbonyl complexes and very close to r_e(CO) in the CO monomer. (ii) The AuC bonds are relatively long. Both r(CO) and r(AuC) are consistent with small metal−CO π-back-donation to the π^*(CO) antibonding orbital. (iii) There is a trend to decreasing Au−C bond length in the sequence OC−AuBr > OC−AuCl > OC−AuF, with this bond in OC−AuF very much shorter than in the other two molecules. This trend is reproduced by the MP2 results in Table 4.

Table 5. Comparison of M−C and C−O Bond Lengths (Å)

	M−C	C−O	comments
OC−AuF	1.847	1.134	FTMW, this work (r_0 struct)
OC−AuCl	1.8829	1.1323	FTMW, this work (r_s struct)
OC−AuBr	1.8917	1.1321	FTMW, this work (r_s struct)
OC−Pt	1.760	1.148	FTMW[43] (r_s struct)
OC−Ni	1.687	1.166	CCSD[T][44]
OC−Fe	1.727	1.1598	FTMW[45]
$(OC)_4$–Ni	1.838	1.141	electron diffraction[46]
$(OC)_5$–Fe	1.833	1.145	electron diffraction[47]
C−O		1.128	r_e value[5]

Vibrational Wavenumbers and Vibrational Satellites

For OC−AuCl, lines from excited vibrational states were observed for several isotopomers. Of all the coinage metal halide complexes whose microwave spectra have been measured thus far, including the noble gas complexes,[11−15] this is only one for which such excited-state transitions have been assigned. OC−AuF produced only ground-state lines, and candidates for OC−AuBr were too weak to be assigned. It is thus of interest to consider which normal mode the lines arise from and why.

To start with, OC−AuCl has seven normal modes, two pairs of which are doubly degenerate. The rotational constant B_v of a particular vibrational state is given by

$$B_v = B_e - \sum_i \alpha_i \left(v_i + \frac{d_i}{2} \right) \qquad (10)$$

where B_e is the equilibrium rotational constant, α_i is the vibration−rotation constant for the ith normal mode of degeneracy d_i, and v_i is the vibrational quantum number. From eq 10, using the rotational constants in Table 1, we get $\alpha_i \sim +2.83$ MHz. The positive sign (plus lack of l-type doubling) indicates that the excited state lines are from a parallel, stretching mode, thus eliminating the two bending modes as candidates. Since the vibrational temperature is probably ∼200 K in the supersonic expansion the high-frequency CO stretch is also unlikely, by the Boltzmann law.

This leaves the AuC and AuCl stretching modes. Antes et al.[24] predicted them to be at 460 and 375 cm^{-1}, respectively; our calculation using a larger basis set for the Au atom predicts them to be at 474 and 407 cm^{-1}, respectively (Table 6). Although the nearness of their frequencies suggests possible considerable AuC/AuCl mixing, Antes et al. found this to be minimal: 93/4 for the 460 cm^{-1} mode (AuC stretch), and 1/99 for the 375 cm^{-1} mode (AuCl stretch). Assignment to one or other of the valence stretches is thus reasonable, despite the nearness of the frequencies.

Several experimental observations favor an assignment to the Au−C stretch: (1) When argon was used as the backing gas, no lines of vibrationally excited AuCl monomer were observed, even though excited-state lines of the complex were found. (2) No lines of the excited AuCl stretch were observed for Ar−AuCl. (3) When neon was used as the backing gas, the intensities of the excited vibrational state lines of monomeric AuCl were greatly reduced on addition of 1.5% CO to the Ne/Cl_2 gas mixture. Overall the evidence is strong but not conclusive that the excited state is that of the Au−C stretch.

(41) Watson, J. K. G.; Roytburg, A.; Ulrich, W. *J. Mol. Spectrosc.* **1999**, *196*, 102.
(42) Evans, C. J.; Gerry, M. C. L. *J. Am. Chem. Soc*. **2000**, *122*, 1560.
(43) Evans, C. J.; Gerry, M. C. L. *J. Phys. Chem.* **2001**, in press.
(44) Solupe, M.; Bauschlicher, C. W., Jr.; Lee, T. J. *Chem. Phys. Lett.* **1992**, *189*, 266.
(45) Kasai, Y.; Obi, K.; Ohshima, Y.; Endo, Y.; Kawaguchi, K. *J. Chem. Phys.* **1995**, *103*, 90.
(46) Hedberg, L.; Iijuma, T.; Hedberg, K. *J. Chem. Phys*. **1979**, *70*, 3224.
(47) Beagley, B.; Cruickshank, D. W. J.; Pinder, P. M.; Robiette, A. G.; Sheldrick, G. M. *Acta Crystallogr*. **1969**, *B25*, 737.
(48) O'Brien, L. C.; Elliott, A. L.; Dulick, M. *J. Mol. Spectrosc.* **1999**, *194*, 124.
(49) McIntosh, D.; Ozin, G. A. *Inorg. Chem*. **1977**, *16*, 51.
(50) Willner, H.; Aubke, F. *Inorg. Chem*. **1990**, *29*, 2195.

Table 6. Vibrational Frequencies (cm^{-1})

	method	Π XAuC def	Σ^+ AuX str	Π OCAu def	Σ^+ CAu str	Σ^+ CO
OCAuCl	MP2	86	407	436	474	2145
	MP2[24]	81	375	420	460	2138
	IR[18]	95	371	416	443	2162
	Raman[18]	96	358	399	423	2183
	IR[19]					2153
	diatomic approx		406			
OCAuF	MP2	126	626	482	502	2154
	diatomic approx				516	
OCAuBr	MP2	80	279	428	468	2143
	diatomic approx		292			
	IR[19]					2151
AuCl	MP2		395			
	electronic[48]		383			
	FTMW[37]		383			
AuF	MP2		548			
AuBr	MP2		275			
	FTMW[37]		264			
AuCO	IR[49]					2039.4
$Au(OSO_2F)(CO)$	IR[50]					2198
CO	MP2					2136.1
	IR[5]					2138

The centrifugal distortion constants also contain vibrational information. With the noble gas complexes[11−15] it was possible to obtain reasonable estimates of the noble gas−Au stretching frequencies with the AuX moiety approximated as being a rigid unit. The same approximation was attempted here, using the equation[51]

$$\omega \approx \left(\frac{4B_0^3}{D_J}\right)^{1/2} \qquad (11)$$

The results were 516 cm^{-1} for OC−AuF, 406 cm^{-1} for OC−AuCl, and 292 cm^{-1} for OC−AuBr. Only for OC−AuF is there any agreement with ν(Au−C) from the MP2 calculation (Table 6). However, for OC−AuCl and OC−AuBr there is remarkable agreement with the MP2 values for ν(AuCl) and ν(AuBr), respectively. Perhaps this is not so surprising, since for both these complexes these two frequencies are lower than ν(AuC) and eq 11 does not discriminate between the modes. In effect, for these two complexes the diatomic approximation would seem to apply with the assumption that the OCAu moiety is rigid.

Nuclear Quadrupole Coupling Constants

The spectra of all three complexes contain hyperfine structure arising from interactions of the rotational angular momenta with the nuclear spin angular momenta of Au, Cl, and Br. The predominant mechanism is nuclear quadrupole coupling, which arises through an electric field gradient (EFG) at the nucleus and gives a measure of the electron distribution in, and hence the bonding of, the atom in question. The parameters giving this measure are the nuclear quadrupole coupling constants (NQCC). If there is any significant variation in the electronic structure, as for example in the formation of a new chemical bond, then changes will occur in the EFGs at the quadrupolar nuclei, and these will be reflected in their NQCCs.

The resolution of the experiments was high enough that in some cases a magnetic interaction between the rotation and nuclear spins was also observed. This interaction was very weak, and its derived constants C_I, the nuclear spin−rotation constants, were poorly determined. It will not be considered further.

(a) Au Nuclear Quadrupole Coupling. Table 7 contains the Au NQCCs for a number of Au(I) species, including the OC−AuX (F, Cl, Br) complexes. Also included in Table 7 are some Au NQCCs for related systems, obtained using Mössbauer spectroscopy.[21,52,53] There are many notable points of comparison.

Table 7. Nuclear Quadrupole Coupling Constants (MHz) of Au, Cl, and Br

molecule/X	F	^{35}Cl	^{79}Br	I
Au Coupling Constants				
AuX(g, FTMW)	−53.23[a]	9.6331[b]	37.267[b]	78.27[c]
AuX(s, Mössbauer)		(−)579.8[d]	(−)527.4[d]	
Ar−AuX	−333.4[e]	−259.8[f]	−216.7[e]	
Kr−AuX		−349.9[f]		
AuX_2^-(Mössbauer)		(−)765[g−i]	(−)790[I,j]	
OC−AuX(g, FTMW)	−1006.3	−1026.0	−999.1	
OC−AuX(s, Mössbauer)		(−)916[g]		
Halogen Coupling Constants				
AuX(g, FTMW)		−61.99[b]	492.3[b]	−1707.9[c]
Ar−AuX		−54.05[f]	428.5[e]	
Kr−AuX		−52.01[f]		
AuX_2^-(Mössbauer)		(−)35[g−i]	202.3[I,j]	
OC−AuX(FTMW)		−36.39	285.09	

[a] Reference 42. [b] Reference 37. [c] Reference 30. [d] Reference 52. [e] Reference 14. [f] Reference 13. [g] Reference 21. [h] Reference 54. [i] Reference 55. [j] Reference 56.

To start with, there is a major variation in the values for the AuX *monomers*, including a sign change.[30,37,42] There are, furthermore, substantial differences between the FTMW and Mössbauer-derived values for AuCl and AuBr. These differences arise because in the solid phase the gold monohalides form zigzag chains [···X−Au−X−Au···]. Unfortunately, interpreting NQCCs and relating them to bonding in a molecule are extremely difficult to do for transition-metal-containing species, especially for the heavier metals such as Au, where d and f orbitals, as well as relativistic effects, can play a major role in the bonding.[37,57]

(51) Kratzer, A. *Z. Phys*. **1920**, *3*, 289.
(52) McAuliffe, C. A.; Parish, R. V.; Randell, P. D. *J. Chem. Soc., Dalton Trans.* **1977**, 1426.
(53) Jones, P. G.; Williams, A. F. *J. Chem. Soc., Dalton Trans.* **1977**, 1430.
(54) Bowmaker, G. A.; Whiting, R. *Aust. J. Chem.* **1976**, *29*, 1407.
(55) Viegers, T. P. A.; Trooster, J. M.; Bouten, P.; Rit, T. P. *J. Chem. Soc., Dalton Trans.* **1977**, 2074.
(56) Bowmaker, G. A.; Boyde, P. D. W.; Sorrenson, R. J. *J. Chem.Soc., Faraday Trans.* **1985**, *81*, 1627.
(57) Pernpointner, M.: Schwerdtfeger, P.; Hess, B. A. *Int. J. Quantum Chem*. **2000**, *76*, 371.

The formation of complexes causes major changes in the Au NQCCs. These changes are strong indicators of formation of new chemical bonds even when the ligands are noble gases,[12−14] where the changes in NQCCs take their values roughly one-third of the way to those of isoelectronic AuX_2^- ions. When CO is the ligand, the changes are much greater and carry the values well beyond those of the ions. This is perhaps to be expected because OC−Au coordination is of a much higher bond order than noble gas−Au coordination. There is a difference, however, in the Au NQCC trends on varying the halides. For the Ar−AuX the Au NQCCs increase (become less negative) in the order X = F < Cl < Br with the differences between the complexes roughly paralleling those of the AuX monomers. This trend is not followed, however, for OC−AuX: although it is maintained for OC−AuCl and OC−AuBr, the value for OC−AuF is between those of the other two complexes, providing further evidence that OC−AuF is rather different.

In contrast to AuX, there is some agreement between the NQCCs of OC−AuCl from FTMW and Mössbauer spectroscopy.[11] However, the crystal structure of OC−AuCl shows it to contain linear monomers, with the shortest Au...Au separation being 3.38 Å.[20] It is thus reasonable that the two values are comparable.

(b) Cl and Br Nuclear Quadrupole Coupling. It is seen from Table 6 that the magnitudes of the NQCC of Cl and Br decrease very considerably from their monomeric values. The changes are comparable to, though somewhat less than, those on formation of AuX_2^- (X = Cl or Br) from the monomers. They are considerably greater than the changes on formation of noble gas−AuX.

Antes et al.[24] predicted the Cl electric field gradients (EFGs) of AuCl and OCAuCl as −2.804 and −1.827 au, to give ^{35}Cl NQCC values of −53.7 and −35.0 MHz, respectively. Though the agreement with experiment is excellent for the complex, it is rather poorer for the monomer, so the agreement for the complex may be somewhat fortuitous.

The agreement is even poorer when Mulliken populations from the MP2 calculations described below are used in the Townes−Dailey equation[58,59]

$$eQq(\mathrm{X}) = \left(n_z - \frac{n_x + n_y}{2}\right) eQq_{n10} \qquad (12)$$

where $eQq(X)$ is the NQCC of Cl or Br, eQq_{n10} is the NQCC of a singly occupied np_z orbital (109.74 MHz for X = ^{35}Cl and −769.76 MHz for X = ^{79}Br [59]), and n_x, n_y, and n_z are orbital populations. The predicted values for ^{35}Cl in Au^{35}Cl and OCAu^{35}Cl are −66.9 and −51.4 MHz: both the actual values and the changes are nowhere near the experimental values. For ^{79}Br the corresponding Townes−Dailey values are +596.5 and +554.2 MHz, making the agreement with experiment even worse.

Discussion and Conclusions

The experimental techniques used in this work have proved ideal for preparing and characterizing the OC−AuX complexes (X = F, Cl, Br). There was no difficulty in preparing any of them, even the previously unreported OC−AuF. OC−AuCl is so stable that spectra of excited vibrational states were easily seen (and were so strong as to be initially assigned to the ground vibrational state). To have been able to prepare OC−AuF is especially interesting, for it is only recently that the existence of AuF monomer has been confirmed through its microwave spectrum.[42] However, the molecule Ar−AuF has also proved straightforward to prepare.[14]

Table 8. MP2 Mulliken Orbital Populations for AuX, CO, and XAuCO (X = F, Cl, Br)

	FAuCO	AuF + CO	ClAuCO	AuCl + CO	BrAuCO	AuBr + CO
q^X	−0.37	−0.32	−0.14	−0.13	0.20	0.08
n_s^X	1.99	1.98	1.97	1.98	1.72	1.80
$n_{p\sigma}^X$	1.64	1.54	1.43	1.33	1.18	1.15
$n_{p\pi}^X$	3.72	3.78	3.80	3.88	3.80	3.85
$n_{d\sigma}^X$					2.00	2.00
$n_{d\pi}^X$					4.00	4.00
$n_{d\delta}^X$					4.00	4.00
q^{Au}	0.03	0.32	−0.33	0.13	−0.77	−0.08
n_s^{Au}	0.91	0.60	1.17	0.78	1.64	0.96
$n_{p\sigma}^{Au}$	0.33	0.07	0.38	0.11	0.36	0.15
$n_{p\pi}^{Au}$	0.21	0.15	0.20	0.14	0.17	0.14
$n_{d\sigma}^{Au}$	1.61	1.77	1.70	1.83	1.76	1.86
$n_{d\pi}^{Au}$	3.74	4.00	3.74	3.97	3.75	3.96
$n_{d\delta}^{Au}$	3.96	4.00	3.98	3.96	3.96	3.96
q^C	0.43	0.05	0.55	0.05	0.65	0.05
n_s^C	1.23	1.81	1.22	1.81	1.16	1.81
$n_{p\sigma}^C$	0.87	0.90	0.78	0.90	0.73	0.90
$n_{p\pi}^C$	1.32	1.13	1.32	1.13	1.32	1.13
$n_{d\sigma}^C$	0.03	0.03	0.03	0.03	0.03	0.03
$n_{d\pi}^C$	0.11	0.08	0.10	0.08	0.10	0.08
q^O	−0.09	−0.05	−0.08	−0.05	−0.07	−0.05
n_s^O	1.89	1.81	1.89	1.81	1.89	1.81
$n_{p\sigma}^O$	1.36	1.40	1.36	1.40	1.36	1.40
$n_{p\pi}^O$	2.80	2.80	2.78	2.80	2.78	2.80

Precise geometries have been obtained for all three molecules, though for those obtained using least-squares fits there are sometimes difficulties with correlations among some of the bond lengths, at least in part because isotopic substitutions could not be made at Au. The CO bond lengths are very close to, but probably slightly greater than, that of free CO. The AuC bonds are fairly long. While the AuCl and AuBr distances increase on complex formation, the AuF distance seemingly decreases slightly. Indeed other features of the geometry of OC−AuF differ from those of the other two molecules. The CO distance is slightly (∼0.002 Å) longer, and the AuC distance is significantly (∼0.01 Å) shorter; both features are predicted by the MP2 calculations.

The MP2 calculations have produced some interesting results. To start with, they predict the bond lengths rather well (Table 4), including the significant difference in r(Au−C) between OC−AuF and the other two complexes mentioned above. Universally the MP2 values for r(CO) are ∼0.01 Å too long. For OC−AuCl the present calculations do a slightly better job than the earlier ones.[24] Where comparisons can be made (Table 6), there is similar reasonable agreement between the MP2 and experimental vibration frequencies and, in particular, the lack of change or slight blue shift of ν(CO) when CO is bonded to Au. For all three complexes the Mulliken populations (Table 8) indicated significant σ-donation (∼0.6−0.8 electron) from CO to Au, as well as a small amount of π-back-donation (∼0.2 electron) from Au to CO. This is contrary to the simple picture involving no π−back-bonding normally used to rationalize the slight blue shift of ν(CO) and the relatively long AuC bonds. Our results again corroborate earlier work.[24,25] It seems likely that variations in the parameters result from a subtle combination of several effects, including, for example, the degrees of σ- or π-donation and relative charges at the various atoms in the molecule.[24]

(58) Townes, C. H.; Dailey, B. P. *J. Chem. Phys.* **1949**, *17*, 982.
(59) Gordy, W.; Cook, R. L. Microwave Molecular Spectra, No. XVIII. In *Techniques of Chemistry*, 3rd ed.; Wiley: New York, 1984.

In virtually every measured and calculated property, the complex OC−AuF is significantly different from OC−AuCl and OC−AuBr. The AuC bond is ∼0.04 Å shorter, and the CO bond ∼0.002 Å longer. The calculated AuC and CO stretching frequencies are ∼30 and ∼10 cm^{-1} higher, respectively. The changes in the Au nuclear quadrupole coupling constant on complex formation are −953, −1036, and −1036 MHz for the fluoride, chloride, and bromide, respectively; the change for the fluoride is considerably different than those for the other two compounds. It is difficult to see a simple reason for all these differences, which in some ways are rather contradictory. For example the Au−C distance, being shorter, might suggest a stronger bond, while the change in the Au coupling constant, being less, might suggest less electron displacement and hence a weaker bond. The Mulliken populations (Table 8) are of little help, though it is perhaps significant that the fluoride is the only one of the complexes in which Au has a positive charge. Figure 4a,b shows contours of the electron density in the AuC bonding molecular orbitals of OC−AuCl and OC−AuF, respectively. A very noticeable feature is that there is considerably more electron density in the AuF part of the orbital than in the AuCl part, which may have some bearing on the shorter Au−C bond in the fluoride.

Overall the structural properties of the OC−AuX complexes have turned out pretty much as expected. The short C−O bond and a relatively long Au−C bond follow the same trend as deduced for $Au(CO)_2^+$,[9] though there are differences in detail. There are large changes in the electron distributions on complex formation. The ease with which these complexes were prepared suggests that the corresponding Cu and Ag complexes should be readily available by the same technique, even though only one, OC−CuCl, has been previously reported[22,23] and OC−AgCl is believed to be difficult to prepare.[24] Their structural properties should show similar features. These deductions have turned out to be correct. Spectra of the Cu and Ag derivatives have now been measured; details will be published shortly.[60]

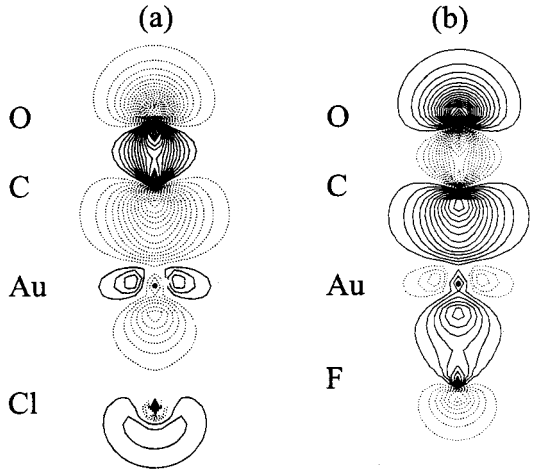

Figure 4. Contour plot of electron density of the Au−C σ-bond for the following: (a) OC−AuCl, contour $0.025 + 0.025n$, $n = 0.18$; (b) OC−AuF, contour $0.025 + 0.025n$, $n = 0.20$.

Acknowledgment. The research has been supported by the Natural Sciences and Engineering Research Council (NSERC) of Canada and by the Petroleum Research Fund, administered by the American Chemical Society.

Supporting Information Available: Tables of measured rotational transition frequencies of OC−AuX (X = F, Cl, Br). This material is available free of charge via the Internet at http://pubs.acs.org.

IC0104407

(60) Walker, N. R.; Gerry, M. C. L. *Inorg. Chem.* **2001**, in press.